Eclética Química Journal

Original article

revista.iq.unesp.br

| Vol. 47 | special issue 1 | 2022 |

Comparative study of benznidazole encapsulation in boron nitride and carbon nanotubes: A quantum chemistry study

Jeziel Rodrigues dos Santos[1+], Osmair Vital de Oliveira[2], Rafael Giordano Viegas[2], José Divino dos Santos[3], Elson Longo[1]

1. Federal University of Sao Carlos, Center for the Development of Functional Materials, São Carlos, Brazil.
2. Federal Institute of Education Science and Technology of São Paulo, Catanduva, Brazil.
3. Goiás State University, Department of Chemistry, Anápolis, Brazil.

+Corresponding author: Jeziel Rodrigues dos Santos, **Phone:** +5562981791374, **Email address:** prof.jeziel@gmail.com

ARTICLE INFO

Article history:
Received: July 19, 2021
Accepted: October 19, 2021
Published: April 11, 2022

Section Editors: Elson Longo and Juan Manuel Andrés Bort

Keywords:
1. BNNT
2. CNT
3. benznidazole
4. encapsulation
5. chagas disease
6. DFT

ABSTRACT: Quantum chemistry methods were used to study boron nitride and carbon nanotubes as possible carriers of antichagasic benznidazole to improve their water solubility and bioavailability. Structurally, no significant changes were observed in both nanotubes throughout the encapsulation process. For the BNZ@BNNT complex, it was possible to notice short interactions, at 0.215 nm, between the hydrogen atoms of the BNZ and the nitrogen atoms of the BNNT. The binding energy reveals that both nanotubes are capable of encapsulating BNZ in an aqueous medium, with values of –71.79 and –62.68 kcal/mol for the BNZ@BNNT and BNZ@CNT complexes. The enthalpy of solvation indicates that the complexes are soluble in water with values of –32.35 and –28.76 kcal mol–1 for the BNZ@BNNT and BNZ@CNT complexes. Regarding chemical stability, Eg and η show that BNZ@BNNT has greater stability (Eg/η of 3.35/1.68 eV) than BNZ@CNT (0.16/0.08 eV). Overall, our results demonstrate that BNNT is a better candidate to be used as a carrier of BNZ than CNT due to its greater structural and chemical stability.

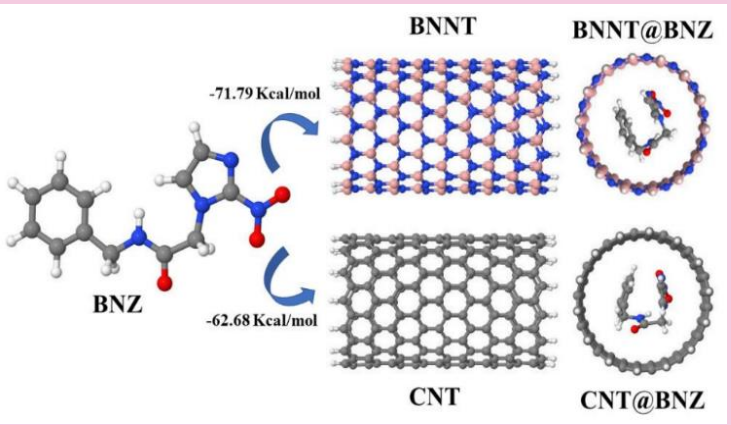

Eclética Química Journal, vol. 47, special issue 1, 2022, 50-56
ISSN: 1678-4618
DOI: 10.26850/1678-4618eqj.v47.1SI.2022.p50-56

1. Introduction

Chagas disease is caused by the protozoan *Trypanosoma cruzi*, which is transmitted mainly by the hematophagous vector insect popularly known as kissing bug. This insect belongs to the order *Hemiptera* and family *Reduviidae* and it is usually found around rock and wood piles and in cracks and gaps of walls and roofs, for instance. This disease is mainly transmitted by the bite of the kissing bug, but it can also be transmitted by blood transfusion and congenital transmission. Some of the efficient ways that have been widely used to control Chagas disease are environmental control and application of insecticides.

Although this disease was discovered in 1909 by the sanitary physician Carlos Chagas, until nowadays there are only two drugs that can treat it: benznidazole and nifurtimox. However, both drugs have low efficiency and strong side effects (Coura and Castro, 2002) presenting an inhibitory activity only in the acute phase of the disease. Additionally, in Brazil, the commercialization of the drug nifurtimox is prohibited (Fairlamb, 1999). It must be emphasized that, according to data obtained from the World Health Organization (WHO), Chagas disease still causes approximately 10,000 deaths per year. Although benznidazole is still in use, it has some limitations such as low water solubility and low permeability. Therefore, high doses of this drug are required to achieve therapeutic efficacy, which consequently increases its toxicity and side effects. A strategy commonly adopted in the literature to overcome these limitations is the use of encapsulating agents, which has been used as drug carriers of antichagasic drugs, such as nanoemulsions (E. Oliveira *et al.*, 2017; Streck *et al.*, 2019; Vermelho *et al.*, 2018), polymeric nanoparticles (Seremeta *et al.*, 2019; Silva *et al.*, 2019), liposomes (Morilla *et al.*, 2002; Vinuesa *et al.*, 2017) and cyclodextrins (Lyra *et al.*, 2012; Melo *et al.*, 2013; Soares Sobrinho *et al.*, 2011) among others.

Even though carrier agents are efficient, the elaboration and development of new nanocarriers have a high experimental cost. Computational chemistry then emerges as a relatively low-cost tool to assist researchers in the optimization of experiments, reducing operating costs. In this sense, O. Oliveira and Viegas (2020), recently used computational chemistry methods to show that cucurbit[7]uryl is a possible new carrier agent of benznidazole. Carbon nanotube (CNT) is another class of nanocarriers that have been extensively studied over the past two decades. In addition to their electrical and optical properties (Rathod *et al.*, 2019), CNTs are also inert and chemically stable (Anzar *et al.*, 2020), which increases their potential application in drug delivery. For such reasons, CNTs have been used as drug carriers in the treatment of different diseases (Wang and Moriyam, 2011). Another nanotube of great interest is the boron nitride nanotube (BNNT). Despite having similar properties, CNTs are metallic or semiconductor, while BNNTs are electrically insulating (Kim *et al.*, 2018). Like CNTs, BNNTs have also been widely used in drug delivery (Ciofani, 2010). Regarding the toxicity, the BNNTs are nontoxic and biocompatible, while possible cytotoxicity of CNTs have been observed (Dehaghani *et al.*, 2020).

From a theoretical point of view, quantum chemistry methods have been adopted to study the encapsulation of different drugs in these nanotubes. For example, both CNT and BNNT have been used to encapsulate anticancer (Azarakhshi *et al.*, 2021; Mahdavifar and Moridzadeh, 2014; Shayan and Nowroozi, 2018; Zaboli *et al.*, 2020) and anti-HIV (Xu *et al.*, 2018) drugs, among others. Recently, CNT (10,10) was used to encapsulate 1,4-dihydropyridine derivatives (Dutra *et al.*, 2017) using the density functional theory. In another study, pure and silicon-doped BNNT (12,0) were employed to adsorb sarin (Santos *et al.*, 2020). In the present work, we propose the use of quantum chemistry methods to study the encapsulation of benznidazole in CNT and BNNT nanotubes in zigzag form (14,0) aiming to improve its bioavailability in the body. It should be noted that until the present moment the use of these nanotubes for the encapsulation of such antichagasic agent has not been reported in the literature.

2. Materials and Methods

The BNNT and CNT zigzag models (14.0) with diameters of 11.78 and 11.06 Å, respectively, were used as a model vehicle to study the BNZ@BNNT and BNZ@CNT complexes. The BNNT and CNT structures were generated using a script (see Supplementary Material S1) with chiral vectors m (18) and n (0) and length of 18.06 and 17.83 Å, respectively. To avoid the effects caused by the ends of the nanotubes, both ends of each nanotube were hydrogenated (Fig. 1). In order to construct the molecular geometry of the BNZ@BNNT and BNZ@CNT complexes, a translational script was used to center the BNZ inside the nanotubes (Supplementary Material S2). The molecular geometry of the BNZ was built through its internal coordinates, considering bond length, bond angle and twist angle. This information was later converted into Cartesian coordinates with the aid of the Molden (Schaftenaar and Noordik, 2000), which is a free code package for structural visualization.

ISSN: 1678-4618
DOI: 10.26850/1678-4618eqj.v47.1SI.2022.p50-56

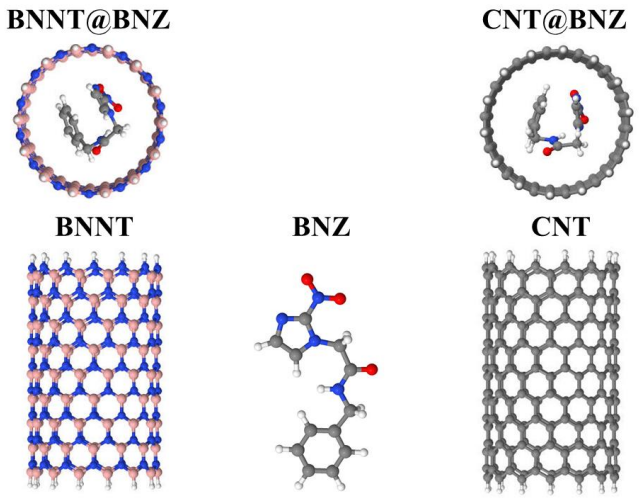

Figure 1. Optimized structures with the DFT-GD3//B3LYP/6-31G(d) method. Oxygen in red, carbon in grey, hydrogen in white, nitrogen in blue, and boron in salmon.

The models (BNNT, CNT and BNZ) and the complexes (BNZ@BNNT and BNZ@CNT) were initially optimized with the PM7 Hamiltonian using the MOPAC2016 program (Stewart, 2016). Subsequently, the structures with minimum energies were reoptimized through DFT, with B3LYP hybrid functional and 6-31G(d) basis function (Rassolov *et al.*, 2001). This theory level was chosen to balance the computational cost and quality of results. The dispersion interaction correction was taken into account by employing the Grimme method (GD3) (Grimme *et al.*, 2010). The stationary points were characterized as a minimum point of energy through harmonic vibrational states, whose imaginary frequencies were not observed. DFT calculations were performed in vacuum and in solvent medium (H_2O) using the PCM method (Scalmani and Frisch, 2010) for the dielectric constant of H_2O and the Gaussian 09 computational package. The natural orbital bonding (NBO) method (Reed *et al.*, 1985) was used to calculate atomic charges. The binding energy (E_{bind}) and the enthalpy of solvation (H_{solv}) of the complexes in vacuum and in solvent medium were calculated using Eqs. 1 and 2, respectively.

$$E_{bind} = E_{NT-BNZ} - (E_{NT} + E_{BNZ}) \quad (1)$$

$$H_{solv} = E_{NT-BNZ-solv} - E_{NT-BNZ-vaccum} \quad (2)$$

where $E_{NT\text{-}BNZ}$ is the total energy of the complexes (BNZ@BNNT and BNZ@CNT), considering the calculations for the vacuum and the solvent medium, E_{NT} is the total energy of the studied nanotubes (BNNT and CNT), E_{BNZ} is the total energy of the BNZ molecule and $E_{NT\text{-}BNZ\text{-}solv}$ are the total energies of the complexes obtained in the solvent and gas phases, respectively.

3. Results and discussion

The encapsulation of BNZ in the BNNT (14.0) and CNT (14.0) was investigated herein using theoretical methods to obtain a new drug delivery system to be used in Chagas disease. Figure 1 presents the most stable geometries obtained for the studied models in aqueous media, using the dielectric constant of water for taking into account the solvent medium.

As it can be seen in Fig. 1, no significant structural change was observed in the BNNT and CNT after the encapsulation process. The main structural differences found in the BNZ molecule are in agreement with the lower root mean square deviation values (RSMD) (< 0.765 nm), which were calculated from the superposition between the unencapsulated and encapsulated BNZ molecule. For the formed complexes, it was possible to observe hydrogen interactions of the order of 0.215 nm between the hydrogen atoms present in the BNZ molecule and the nitrogen atoms from the BNNT nanotube. These interactions provided great stability to the BNZ@BNNT complex when compared to the BNZ@CNT, which is in accordance with the results in Tab. 1, that were calculated from Eq. 1.

To better understand the energetic processes involved in the encapsulation process, the electronic structures for the model vehicles, as well as for the formed complexes, are presented and discussed. The electronic properties were used to clarify the interaction between the BNZ molecule and the inner surface of the BNNT and the CNT model vehicles. The reactivity parameters were based on the energies of molecular orbitals occupied with the highest energy (HOMO, E_{HOMO}) and those unoccupied with the lowest energy (LUMO, E_{LUMO}). According to the Koopmans' theorem (Koopmans, 1934), the ionization potential (IP) is the negative of the HOMO energy ($-E_{HOMO}$), while the electron affinity (EA) can be approximated by the negative of the LUMO energy ($-E_{LUMO}$). The energy gap is another property obtained from the energies of E_{HOMO} and E_{LUMO}, being defined as the absolute difference ($|E_{HOMO} - E_{LUMO}|$). Table 1 summarizes the electronic properties obtained in our calculations.

Eclética Química Journal, vol. 47, special issue 1, 2022, 50-56
ISSN: 1678-4618
DOI: 10.26850/1678-4618eqj.v47.1SI.2022.p50-56

Table 1. Electronic properties obtained from DFT-GD3//B3LYP/6-31G(d) calculations.

Compounds	E_{bind} kcal/mol	H_{solv} kcal/mol	E_{HOMO} eV	E_{LUMO} eV	E_g eV	IP eV	EA eV	Dipole Debye
BNZ/(vacuum)	-	–12.72	–7.04	–2.52	4.52	7.04	2.52	7.81
BNZ/(solvent)	-		–6.72	–2.71	4.01	6.72	2.71	9.98
BNNT/(vacuum)	-	–28.19	–6.37	–0.29	6.08	6.37	0.29	23.81
BNNT/(solvent)	-		–6.28	–0.37	5.91	6.28	0.37	31.99
CNT/(vacuum)	-	–10.41	–3.80	–3.64	0.16	3.80	3.64	0.09
CNT/(solvent)	-		–3.82	–3.66	0.16	3.82	3.66	0.10
BNZ@BNNT/(vacuum)	–80.36	–32.35	–6.29	–2.96	3.33	6.29	2.96	19.38
BNZ@BNNT/(solvent)	–71.79		–6.26	–2.91	3.35	6.26	2.91	23.44
BNZ@CNT/(vacuum)	–69.05	–28.76	–3.80	–3.64	0.16	3.80	3.64	0.16
BNZ@CNT/(solvent)	–62,68		–3.83	–3.67	0.16	3.83	3.67	7.10

Table 2. Quantum molecular descriptors were obtained through the reactivity parameters E_{HOMO} and E_{LUMO} using DFT-GD3//B3LYP/6-31G(d) calculations.

Compounds	μ eV	χ eV	η eV	ω eV	S eV
BNZ (vacuum)	–7.48	7.48	2.26	4.84	0.22
BNZ (solvent)	–4.72	4.72	2.01	1.82	0.25
BNNT (vacuum)	–3.33	3.33	3.04	0.89	0.16
BNNT (solvent)	–3.33	3.33	2.96	0.91	0.17
CNT (vacuum)	–3.72	3.72	0.08	3.49	6.25
CNT (solvent)	–3.74	3.74	0.08	3.51	6.25
BNZ@BNNT (vacuum)	–4.63	4.63	1.67	2.23	0.25
BNZ@BNNT (solvent)	–4.59	4.59	1.68	2.19	0.30
BNZ@CNT (vacuum)	–3.72	3.72	0.08	3.49	6.25
BNZ@CNT (solvent)	–3.75	3.75	0.08	3.52	6.25

In addition, quantum molecular descriptors can be used to better understand the interactions between BNZ and the model vehicles. For this, the global hardness (η), electronegativity (χ), electronic chemical potential (μ), electrophilicity index (ω) and softness chemistry (S) were calculated from Eqs. 3–7, respectively (Koopmans, 1934; Lobo *et al.*, 2020; Serhan *et al.*, 2020; Sheikhi *et al.*, 2018). For instance, μ measures the evasion affinity of a molecule from chemical equilibrium, η measures the charge transfer and the chemical reactivity of a molecule, χ is the capacity of a molecule to attract electrons, and ω is the electrophilic power of a molecule. Furthermore, the stability of molecular systems is related to hardness (η), which is a tool to understand chemical reactivity (Khaleghian and Azarakhshi, 2019). All these quantum descriptors are displayed in Tab. 2.

$$\eta = \frac{I-EA}{2} \quad (3)$$

$$\chi = \frac{I+EA}{2} \quad (4)$$

$$\mu = \frac{-I+EA}{2} \quad (5)$$

$$\omega = \frac{\mu^2}{2} \quad (6)$$

$$S = \frac{1}{2\eta} \quad (7)$$

As shown in Tab. 2, the global hardness value (η) for the BNNT is 3.04 eV in vacuum and 2.96 eV in solvent medium. However, after the formation of the BNZ@BNNT complex, these values change to 1.67 eV in vacuum and 1.68 eV in solvent medium, i.e., the η value of the BNNT decreases as it interacts with the BNZ molecule. These values are greater than those for the BNZ@CNT system, where the η value is practically unchanged (Tab. 2). This is in agreement with the energy of formation of the complexes, as shown in Tab. 1. The electrophilicity index (ω) calculation reveals that the BNZ@BNNT has higher values than the BNZ and isolated BNNT in the solvent phase, thus implying that this complex has a better electrophilic characteristic. Nevertheless, when comparing both complexes, it is possible to observe that, in aqueous media, the BNZ@CNT (3.52 eV) acts as an electrophile due to its high ω value in comparison with the BNZ@BNNT (2.19 eV). In contrast, the lower value of electronegativity (χ) of the BNZ@CNT (3.75 eV)

Eclética Química Journal, vol. 47, special issue 1, 2022, 50-56
ISSN: 1678-4618
DOI: 10.26850/1678-4618eqj.v47.1SI.2022.p50-56

compared to the BNZ@BNNT (4.59 eV) shows that it acts as a nucleophile in solvent phase. The same conclusion can be reached using the μ and η descriptors, being the electrophile characterized by a high value of μ and a low value of η, whereas the opposite is true for the nucleophile.

The dipole moment values of the model vehicles are altered according to the interaction between the BNZ molecule and their internal surfaces (Tab. 1). The change in dipole moment after interaction indicates a charge transference between the BNZ molecule and the BNNT and CNT model vehicles. For better visualization of this process, Fig. 2 illustrates the molecular electrostatic potential (MEP) for the studied compounds.

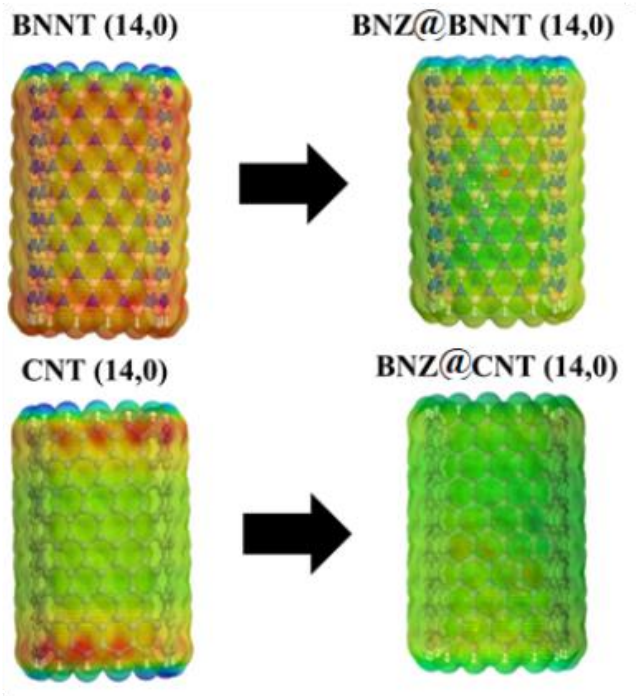

Figure 2. Representation of the molecular electrostatic potential (MEP, in eV) of the BNNT and CNT model vehicles, and the BNZ molecule. For MPE, the negative and positive charges range from red to blue, respectively (for interpretation of the color references in this legend, please refer to the web version of this article).

As it can be seen in Fig. 2, charge transfers can be evidenced by the modification in the MEP after the formation of the BNZ@BNNT and BNZ@CNT complexes. Therefore, according to Tabs. 1 and 2, this transfer process is very important to improve the electronic properties of the studied nanotubes.

4. Conclusions

Chags disease, caused by the protozoan *Trypanosoma cruzi*, was discovered in 1909 by Carlos Chagas. Although this disease is responsible for nearly 10.000 deaths per year worldwide, there is only one effective drug against it: benznidazole (BNZ). However, it has low water solubility and low bioavailability in the organism. Therefore, herein we used quantum chemistry methods to characterize two nanotubes (BNNT and CNT) to be used as carrier agents for the BNZ. The optimized structures of the complexes showed that the presence of BNZ inside the nanotubes did not alter their structural form, which is desired in drug delivery. The binding energy (E_{bind}) revealed that the BNNT and CNT are able to encapsulate BNZ with E_{bind} values of –71.79 and –62.68 kcal mol^{-1} for the BNZ@BNNT and BNZ@CNT complexes, respectively, in aqueous media. The solvation enthalpy of –32.35 and –28.76 kcal mol^{-1} for the BNZ@BNNT and BNZ@CNT complexes, respectively, indicated that they are soluble in water. Additionally, the energy gap (E_g) and global hardness (η) showed that the BNZ@BNNT presents higher stability, with (E_g/η) value of 3.35/1.68 eV against 0.16/0.08 eV for the BNZ@CNT. The electrophilicity index (ω) and electronegativity (χ) values indicated that the BNZ@BNNT and BNZ@CNT act as nucleophile and electrophile, respectively, in aqueous media. Finally, the present results demonstrate that the BNNT is a better candidate to be used as a carrier agent for BNZ than the CNT due to its higher chemical stability, lower binding energy and lower solvation enthalpy.

Authors' contribution

Conceptualization: Santos, J. R.; Oliveira, O. V.; Viegas, R. G.
Data curation: Santos, J. R.; Santos, J. D.
Formal Analysis: Santos, J. R.; Santos, J. D.; Oliveira, O. V.; Viegas, R. G.; Longo, E.
Funding acquisition: Not applicable.
Investigation: Santos, J. R.; Santos, J. D.; Oliveira, O. V.; Viegas, R. G.; Longo, E.
Methodology: Santos, J. R.; Santos, J. D.
Project administration: Oliveira, O. V.; Longo, E.; Santos, J. D.
Resources: Longo, E.; Santos, J. D.
Software: Santos, J. R.; Santos, J. D.
Supervision: Longo, E.
Validation: Santos, J. R.; Santos, J. D.; Oliveira, O. V.; Viegas, R. G.; Longo, E.

Eclética Química Journal, vol. 47, special issue 1, 2022, 50-56
ISSN: 1678-4618
DOI: 10.26850/1678-4618eqj.v47.1SI.2022.p50-56

Visualization: Santos, J. R.; Santos, J. D.; Oliveira, O. V.; Viegas, R. G.; Longo, E.
Writing – original draft: Santos, J. R.; Oliveira, O. V.; Viegas, R. G.
Writing – review & editing: Santos, J. R.; Oliveira, O. V.; Viegas, R. G.

Data availability statement

The data will be available upon request.

Funding

Not applicable.

Acknowledgments

This research was carried out with the support of the Center for High Performance Computing at the State University of Goiás. Jeziel Rodrigues dos Santos thanks CAPES for providing a research grant.

References

Anzar, N.; Hasan, R.; Tyagi, M.; Yadav, N.; Narang, J. Carbon nanotube: A review on synthesis, properties and plethora of applications in the field of biomedical science. *Sensors Int.* **2020**, *1*, 100003. https://doi.org/10.1016/j.sintl.2020.100003

Azarakhshi, F.; Sheikhi, M.; Shahab, S.; Khaleghian, M.; Sirotsina, K.; Yurlevich, H.; Novik, D. Investigation of encapsulation of Talzenna drug into carbon and boron-nitride nanotubes [CNT(8,8-7) and BNNT(8,8-7)]: A DFT study. *Chem. Pap.* **2021**, *75*, 1521–1533. https://doi.org/10.1007/s11696-020-01407-8

Ciofani, G. Potential applications of boron nitride nanotubes as drug delivery systems. *Expert Opin. Drug Deliv.* **2010**, *7* (8), 889–893. https://doi.org/10.1517/17425247.2010.499897

Coura, J. R.; Castro, S. L. A critical review on Chagas disease chemotherapy. *Mem. Inst. Oswaldo Cruz* **2002**, *97* (1), 3–24. https://doi.org/10.1590/S0074-02762002000100001

Dehaghani, M. Z.; Bagheri, B.; Nasiriasayesh, A.; Mashhadzadeh, A. H.; Zarrintaj, P.; Rabiee, N.; Bagherzadeh, M.; Habibzadeh, S.; Abida, O.; Saeb, M. R.; Jang, H. W.; Shokouhimehr, M. Insight into the self-insertion of a protein inside the boron nitride nanotube. *ACS Omega* **2020**, *5* (49), 32051–32058. https://doi.org/10.1021/acsomega.0c05080

Dutra, L. M.; Oliveira, O. V.; Santos, J. D. Computational studies on the encapsulation of 1,4-dihydropyridine derivatives into CNT(10,10). *Aust. J. Chem.* **2017**, *70* (3), 252–257. https://doi.org/10.1071/CH16165

Fairlamb, A. H. Future prospects for the chemotherapy of Chagas' disease. *Medicina (B. Aires)* **1999**, *59* (Suppl. 2), 179–187.

Grimme, S.; Antony, J.; Ehrlich, S.; Krieg, H. A consistent and accurate *ab initio* parametrization of density functional dispersion correction (DFT-D) for the 94 elements H-Pu. *J. Chem. Phys.* **2010**, *132* (15), 154104. https://doi.org/10.1063/1.3382344

Khaleghian, M.; Azarakhshi, F. Theoretical modelling of encapsulation of the Altretamine drug into BN(9,9-5) and AlN(9,9-5) nano rings: A DFT study. *Mol. Phys.* **2019**, *117* (18), 2559–2569. https://doi.org/10.1080/00268976.2019.1574987

Kim, J. H.; Pham, T. V.; Hwang, J. H.; Kim, C. S.; Kim, M. J. Boron nitride nanotubes: Synthesis and applications. *Nano Convergence* **2018**, *5*, 17. https://doi.org/10.1186/s40580-018-0149-y

Koopmans, T. Über Die Zuordnung von Wellenfunktionen Und Eigenwerten Zu Den Einzelnen Elektronen Eines Atoms. *Physica* **1934**, *1* (1–6), 104–113. https://doi.org/10.1016/S0031-8914(34)90011-2

Lobo, J. A. P.; Santos, J. R.; Oliveira, O. V.; Silva, E. L.; Santos, J. D. Theoretical study of greenhouse gases on the zirconium oxide nanotube surface. *Chem. Phys. Lett.* **2020**, *745*, 137236. https://doi.org/10.1016/j.cplett.2020.137236

Lyra, M. A. M.; Soares-Sobrinho, J. L.; Figueiredo, R. C. B. Q.; Sandes, J. M.; Lima, Á. A. N.; Tenório, R. P.; Fontes, D. A. F.; Santos, F. L. A.; Rolim, L. A.; Rolim-Neto, P. J. Study of benznidazole-cyclodextrin inclusion complexes, cytotoxicity and trypanocidal activity. *J. Incl. Phenom. Macrocycl. Chem.* **2012**, *73*, 397–404. https://doi.org/10.1007/s10847-011-0077-5

Mahdavifar, Z.; Moridzadeh, R. Theoretical prediction of encapsulation and adsorption of platinum-anticancer drugs into single walled boron nitride and carbon nanotubes. *J. Incl. Phenom. Macrocycl. Chem.* **2014**, *79*, 443–457. https://doi.org/10.1007/s10847-013-0367-1

Melo, P. N.; Barbosa, E. G.; De Caland, L. B.; Carpegianni, H.; Garnero, C.; Longhi, M.; Fernades-Pedrosa, M. F.; Silva-Júnior, A. A. Host-guest interactions between benznidazole and beta-cyclodextrin in multicomponent complex systems involving hydrophilic polymers and triethanolamine in aqueous solution. *J. Mol. Liq.* **2013**, *186*, 147–156. https://doi.org/10.1016/j.molliq.2013.07.004

Morilla, M. J.; Benavidez, P.; Lopez, M. O.; Bakas, L.; Romero, E. L. Development and *in vitro* characterisation of a benznidazole liposomal formulation. *Int. J. Pharm.* **2002**, *249* (1–2), 89–99. https://doi.org/10.1016/S0378-5173(02)00453-2

Oliveira, E. C. V; Carneiro, Z. A.; Albuquerque, S.; Marchetti, J. M. Development and evaluation of a nanoemulsion containing Ursolic acid: A promising trypanocidal agent: Nanoemulsion with ursolic acid against *T. Cruzi*. *AAPS PharmSciTech* **2017**, *18*, 2551–2560. https://doi.org/10.1208/s12249-017-0736-y

Oliveira, O. V.; Viegas, R. G. Cucurbit[7]uril as a possible nanocarrier for the antichagasic benznidazole: A computational approach. *J. Incl. Phenom. Macrocycl. Chem.* **2020**, *98* (1–2), 93–103. https://doi.org/10.1007/s10847-020-01014-w

Rassolov, V. A.; Ratner, M. A.; Pople, J. A.; Redfern, P. C.; Curtiss, L. A. 6-31G* basis set for third-row atoms. *J. Comput. Chem.* **2001**, *22* (9), 976–984. https://doi.org/10.1002/jcc.1058

Rathod, V.; Tripathi, R.; Joshi, P.; Jha, P. K.; Bahadur, P.; Tiwari, S. Paclitaxel encapsulation into dual-functionalized multi-walled carbon nanotubes. *AAPS PharmSciTech* **2019**, *20*, 51. https://doi.org/10.1208/s12249-018-1218-6

Reed, A. E.; Weinstock, R. B.; Weinhold, F. Natural Population Analysis. *J. Chem. Phys.* **1985**, *83* (2), 735. https://doi.org/10.1063/1.449486

Santos, J. R.; Silva, E. L.; Oliveira, O. V.; Santos, J. D. Theoretical study of sarin adsorption on (12,0) boron nitride nanotube doped with silicon atoms. *Chem. Phys. Lett.* **2020**, *738*, 136816. https://doi.org/10.1016/j.cplett.2019.136816

Scalmani, G.; Frisch, M. J. Continuous surface charge polarizable continuum models of solvation. I. General formalism. *J. Chem. Phys.* **2010**, *132* (11), 114110. https://doi.org/10.1063/1.3359469

Schaftenaar, G.; Noordik, J. H. Molden: A pre- and post-processing program for molecular and electronic structures. *J. Comput. Aided. Mol. Des.* **2000**, *14*, 123–134. https://doi.org/10.1023/A:1008193805436

Seremeta, K. P.; Arrúa, E. C.; Okulik, N. B.; Salomon, C. J. Development and characterization of benznidazole nano- and microparticles: A new tool for pediatric treatment of Chagas disease? *Colloids Surf. B Biointerfaces* **2019**, *177*, 169–177. https://doi.org/10.1016/j.colsurfb.2019.01.039

Serhan, M.; Abusini, M.; Almahmoud, E.; Omari, R.; Al-Khaza'leh, K.; Abu-Farsakh, H.; Ghozlan, A.; Talla, J. The electronic properties of different chiralities of defected boron nitride nanotubes: Theoretical study. *Comput. Condens. Matter* **2020**, *22*, e00439. https://doi.org/10.1016/j.cocom.2019.e00439

Shayan, K.; Nowroozi, A. Boron nitride nanotubes for delivery of 5-fluorouracil as anticancer drug: A theoretical study. *Appl. Surf. Sci.* **2018**, *428*, 500–513. https://doi.org/10.1016/j.apsusc.2017.09.121

Sheikhi, M.; Shahab, S.; Khaleghian, M.; Hajikolaee, F. H.; Balakhanava, I.; Alnajjar, R. Adsorption properties of the molecule resveratrol on CNT(8,0-10) nanotube: Geometry optimization, molecular structure, spectroscopic (NMR, UV/Vis, excited state), FMO, MEP and HOMO-LUMO investigations. *J. Mol. Struct.* **2018**, *1160*, 479–487. https://doi.org/10.1016/j.molstruc.2018.01.005

Silva, A. M. S.; Caland, L. B.; Doro, P. N.M; Oliveira, A. L. C. S. L.; de Araújo-Júnior, R. F.; Fernandes-Pedrosa, M. F.; do Egito, E. S. T.; da Silva-Junior, A. A. Hydrophilic and Hydrophobic Polymeric Benznidazole-Loaded Nanoparticles: Physicochemical Properties and in Vitro Antitumor Efficacy. *J. Drug Deliv. Sci. Technol.* **2019**, *51*, 700–707. https://doi.org/10.1016/j.jddst.2019.04.005

Soares Sobrinho, J. L.; Soares, M. F. de L. R.; Torres Labandeira, J. J.; Alves, L. D. S.; Rolim Neto, P. J. Improving the solubility of the antichagasic drug benznidazole through formation of inclusion complexes with cyclodextrins. *Quim. Nova* **2011**, *34* (9), 1534–1538. https://doi.org/10.1590/S0100-40422011000900010

Stewart Computational Chemistry; Stewart, J. J. P.: Colorado Springs, 2016. http://openmopac.net/ (accessed 2021-04-14)

Streck, L.; Sarmento, V. H. V.; Menezes, R. P. R. P. B. de; Fernandes-Pedrosa, M. F.; Martins, A. M. C.; da Silva-Júnior, A. A. Tailoring microstructural, drug release properties, and antichagasic efficacy of biocompatible oil-in-water benznidazol-loaded nanoemulsions. *Int. J. Pharm.* **2019**, *555*, 36–48. https://doi.org/10.1016/j.ijpharm.2018.11.041

Vermelho, A. B.; Cardoso, V. S.; Ricci Junior, E.; Santos, E. P. dos; Supuran, C. T. Nanoemulsions of sulfonamide carbonic anhydrase inhibitors strongly inhibit the growth of *Trypanosoma cruzi*. *J. Enzyme Inhib. Med. Chem.* **2018**, *33* (1), 139–146. https://doi.org/10.1080/14756366.2017.1405264.

Vinuesa, T.; Herráez, R.; Oliver, L.; Elizondo, E.; Acarregui, A.; Esquisabel, A.; Pedraz, J. L.; Ventosa, N.; Veciana, J.; Viñas, M. Benznidazole nanoformulates: A chance to improve therapeutics for chagas disease. *Am. J. Trop. Med. Hyg.* **2017**, *97* (5), 1469–1476. https://doi.org/10.4269/ajtmh.17-0044

Wang, Q.; Moriyam, H. Carbon nanotube-based thin films: Synthesis and properties. In *Carbon Nanotubes - Synthesis, Characterization, Applications*; IntechOpen, 2011; pp 487–514. https://doi.org/10.5772/22021

Xu, H.; Li, L.; Fan, G.; Chu, X. DFT study of nanotubes as the drug delivery vehicles of Efavirenz. *Comput. Theor. Chem.* **2018**, *1131*, 57–68. https://doi.org/10.1016/j.comptc.2018.03.032

Zaboli, M.; Raissi, H.; Zaboli, M. Investigation of nanotubes as the smart carriers for targeted delivery of mercaptopurine anticancer drug. *J. Biomol. Struct. Dyn.* **2020**, 1–14. https://doi.org/10.1080/07391102.2020.1860823